JOURNAL OF Applied Polymer SCIENCE

Polypropylene membranes modified with interpenetrating polymer networks for the removal of chromium ions

Yesid Tapiero,[1] Bernabé L. Rivas,[1] Julio Sánchez,[1] Marek Bryjak,[2] Nalan Kabay[3]
[1]Polymer Department, Faculty of Chemistry, University of Concepción, Chile
[2]Division of Polymer and Carbon Materials, Wroclaw University of Technology, Wroclaw 50-370, Poland
[3]Department of Chemical Engineering, Ege University, Izmir 35100, Turkey
Correspondence to: B. L. Rivas (E-mail: brivas@udec.cl)

ABSTRACT: Polypropylene (PP) membranes incorporating poly[(ar-vinylbenzyl) trimethylammonium chloride] P(ClVBTA), and poly[-sodium (styrene sulfonate)] P(SSNa) were modified via an "*in situ*" radical polymerization synthesis. Two methods were used for impregnation of the reactive solution: pressure injection and plasma superficial activation with argon gas. The following conditions were varied: the monomer concentrations, number of injections, and cross-linked concentration. The modified polypropylene membranes were then characterized using scanning electron microscopy/energy dispersive X-ray spectroscopy, Fourier transform-infrared spectroscopy, electrokinetic potential, and Donnan dialysis for the chromium ions transport. The modified membranes exhibited a hydrophilic character with a water uptake capacity between 15% and 20% and a percent modification between 2.5% and 4.0%. This was compared with the results of an unmodified polypropylene membrane as the blank and the mentioned polypropylene membrane has not the capacity to uptake water because this kind of material is highly hydrophobic. Hexavalent chromium ions were efficiently transported by the modified membranes containing P(ClVBTA) via a plasma method and it achieved 59.2% extraction at pH 9.0 using a 1-mol L^{-1} NaCl extraction agent. Therefore, unmodified polypropylene membrane shows an extraction percentage close to 10% from the hexavalent chromium ions at pH 9.0. In the same way, the trivalent chromium transport using membranes modified with P(SSNa) achieved 49.0% extraction at pH 2.0 using 1×10^{-1} mol L^{-1} HNO_3 and 1 mol L^{-1} NaCl as the extraction agents. Moreover, the unmodified polypropylene membrane reached a value close to 10% from the trivalent chromium ions using 1×10^{-1} mol L^{-1} HNO_3 and 1 mol L^{-1} NaCl. © 2015 Wiley Periodicals, Inc. J. Appl. Polym. Sci. **2015**, *132*, 41953.

KEYWORDS: adsorption; membranes; separation techniques

Received 24 August 2014; accepted 6 January 2015
DOI: 10.1002/app.41953

INTRODUCTION

Currently, water sources polluted with metallic and metalloid ions cause serious environmental problems. Some water contaminating species include chromium, mercury, copper, nickel, cadmium, and arsenic. Chromium ions in the water present different oxidation states, for example, the trivalent chromium Cr(III) and hexavalent chromium Cr(VI).

Cr(VI) is the more toxic ionic species and causes serious health problems such as cancer. This toxicity depends on the concentration and exposure period.[1,2] Cr(VI) ions are water soluble in all pH range and they accumulate well in biological systems. The World Health Organization (WHO) recommends a maximum concentration limit of 0.05 (mg L^{-1}) for Cr(VI) or the Cr(III).[3]

Cr(VI) ions exist as oxyanions, and their speciation depends on the pH and concentration. Therefore, there is a high quantity of chromate (CrO_4^{2-}) ions at weakly acidic pH values above 6.0; this species can exist as an acid chromate ($HCrO_4^-$) and dichromate ($Cr_2O_7^{2-}$) ion mixture. If the pH is strongly acidic and the Cr(VI) ion are highly concentrated, they exist as dichromate ($Cr_2O_7^{2-}$), chromic acid (H_2CrO_4), and dichromate acid ($H_2Cr_2O_7$).[4,5]

Cr(III) is an essential element for life.[6] Nevertheless, at certain concentrations, it can damage the cell membrane's biological permeability, ionic channels, receptors, and enzymes.[6] The main Cr(III) species that dissolves in water are $Cr(OH)_2^+$, $Cr(OH)_3^0$, and $Cr(OH)_4^-$ chromyl ions, which prevail at pH values below 3.6.[7] When the pH values are higher, Cr(III) precipitates as $Cr(OH)_3 \times nH_2O$.[8]

The most important industries that generate the following Cr(VI) and Cr(III) compounds are paints, both surface plating and chromium electro-plating (decorative and hardplating), stainless steel handwork, and other alloys, concrete industry,

etc.[6,8,9] The techniques for the removal and recovery of Cr(VI) are important for the environmental protection. Also, it is important to the worldwide need for Cr(VI) increase and the grades of ore decrease, the incentive to find more effective and efficient Cr(VI) purification methods is growing. In addition, these industries have used different methods to remove Cr(VI)/Cr(III) ions from polluted solutions.

The most common methods to remove these ions are reduction and precipitation,[10] adsorption,[11] and ion exchange together with functional membranes.[12,13] Membrane technologies allow for reverse osmosis, ultrafiltration, nanofiltration, dialysis, diffusion dialysis, Donnan dialysis, membrane electrolysis, and electrodialysis[5,13–15] (liquid, emulsified and supported).[14,16,17]

Taking into account, the Donnan dialysis uses the chemical potential differences between the membrane sides to generate ionic transport and maintain the electroneutrality of the two solutions.[18] Donnan dialysis has applications in many areas, such as chemical analysis for preconcentration, extraction processes, hydrometallurgy,[19] separating acids from their salts,[20,21] radioactive flow deacidification,[22] removing copper and zinc using commercial cationic membranes,[23] and removing inorganic anions such as fluoride, nitrate, bromated, and borates from drinking water.[15,20,24] In addition, Donnan dialysis has removed Cr(VI) ions using commercial anion exchange membranes such as SB-6470, AFN, ACM, and Raipore 1030.[19,25,26] The development of efficient Donnan dialysis processes depends on selecting a suitable work functional membrane.

An alternative way of modifying the microporous membranes is by the interpenetrating polymer networks (IPN) because it makes possible to develop new materials that have definitive properties. For these reasons, these materials are important in both fundamental and applied investigations. The process is fast and simple way for many polymeric systems.

IPN architectures form when two or more polymer networks are partially and noncovalently crosslinked on the molecular scale. These IPNs cannot be separated by link breakages via chemical methods.[27,28] The purpose of the synthesis of IPNs is to have the ability to combine chemical and physical properties (for example thermal, chemical, and mechanical resistance) into one material.[28,29]

Some applications of IPNs materials are biomedical material applications,[30,31] water sorption materials,[32] enzyme immobilization,[33] ion exchange membranes,[34,35] fuel cells,[36] etc.

Functional IPN membranes are ideally developed from chemically stable commercial porous materials. Some example commercial disposable microporous membranes are polypropylene (MPP) or polyethylene.[24] These polyolefin materials are attractive due to the thermal and mechanical stability and good chemical properties.

On the other hand, the poly[(ar-vinylbenzyl) trimethylammonium chloride] is an effective anion exchange polymer used in removal processes of chromium ions.[9] It is also used as resin, functional part of membrane, and water-soluble polymer for the liquid-phase polymer based retention technique (LPR).[37–40] Also, the poly[sodium (styrene sulfonate)], P(SSNa), is an efficient cation exchange polymer. It is used in the removal of metal cations as a functional resin, active part of membrane, and water-soluble polymer for the liquid-phase polymer based retention technique (LPR).[37,41,42]

The main goal of this work is to modify (MPP) membranes with interpenetrating poly[(ar-vinylbenzyl) trimethylammonium chloride], P(ClVBTA) and poly[sodium (styrene sulfonate)], P(SSNa) networks and study these membranes for Cr(VI) and Cr(III) ion transport via Donnan dialysis.

EXPERIMENTAL

Reagents and Materials

Ar-[(vinylbenzyl)trimethylammonium chloride] (ClVBTA, Aldrich), *N,N′*-methylenebisacrylamide (MBA, Aldrich), sodium styrenesulfonate (SSNa, Aldrich), and ammonium persulfate (APS, Merck) were used for the (IPN) synthesis.

Microporous isotactic polypropylene (MPP) membranes were used (0.6-μm pore size, AN06 Merck Millipore). The other reagents used to modify the membrane surfaces were glutaraldehyde (Ga; Aldrich), 15 kDa polyvinyl alcohol (PVA, Merck), 15 kDa poly(ethyleneimine) (PEI, Aldrich), divinylsulfone (Aldrich), 200 kDa poly(sodium 4-styrenesulfonate) (P(SSNa), Aldrich), ethanol (Merck), and Type I deionized water from a Thermo Fisher TKA scientific.

A UB-10 pH/mV meter from Denver instrument was used to measure the pH solution. A stirred-cell filtration unit (Millipore, model 8050) was used to inject the reactive solution pressure into the PP membrane porous. An aluminum flat-reactor was used for the radical polymerization.

Hydrochloric acid HCl (Merck), nitric acid HNO_3 (Merck), and sodium hydroxide NaOH, (Merck) were used to control the pH. Potassium dichromate $K_2Cr_2O_7$ [C(VI), Merck] and chromium(III) nitrate nonahydrate $Cr(NO_3)_3 \times 9H_2O$ [Cr(III), Merck] were the chromium sources. Sodium chloride NaCl was the extraction reagent. Sodium nitrate $NaNO_3$ (Merck) was used for the binary system.

A Cary 100 scan UV–visible spectrophotometer from Varian was used to directly measure the Cr(VI) and Cr(III) ion concentrations.[43] The Cr(VI) ion was measured at 350 nm in a pH 3.0 solution and at 372 nm in a pH 9.0 solution.[43] The Cr(III) ion concentration was measured at the wavelengths 407 nm and 573 nm for an acidic pH.[43]

Plasma Reactor

A dielectric barrier discharge (DBD) plasma reactor was used to activate the membrane surfaces; the components and operating modes of the DBD were previously published.[44]

Synthesis of P(ClVBTA) and P(SSNa) Interpenetrating Polymer Networks

The membranes were washed with an aqueous mixture of 50% (w/w) ethanol to eliminate all of the wastes and wet the pores. The "*in situ*" free-radical polymerization was performed inside the membrane pores at 70°C for 24 h. Figure 1 shows the ion exchange IPN formation process. Ammonium persulfate, 1 mol %, was used as the radical initiator.

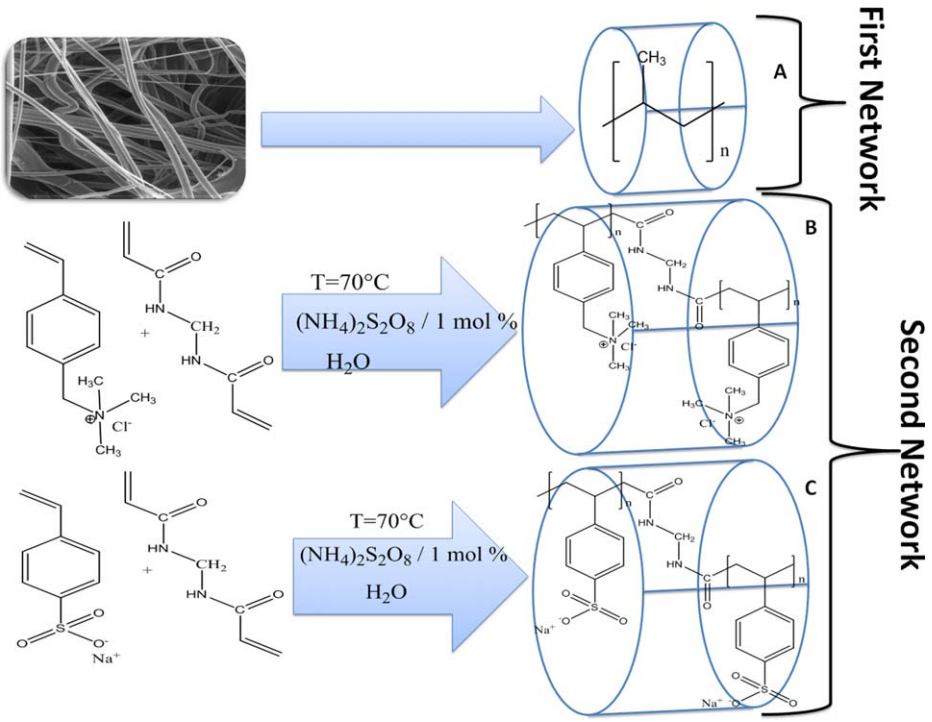

Figure 1. Illustrative diagram of synthesis "*in situ*" of P(ClVBTA) and P(SSNa) IPNs. A. Isotactic polypropylene as first network. B. P(ClVBTA) IPNs. C. P(SSNa) IPNs. [Color figure can be viewed in the online issue, which is available at wileyonlinelibrary.com.]

Interpenetrating Polymer Network Formation via a Pressure Injection and Assisted Plasma Activation

A stirred-cell filtration unit was used with nitrogen gas and a pressure of 1 bar. The functional monomer (ClVBTA or SSNa), crosslinking reagent (MBA), and initiator reagent (APS) in a 10 mL reaction solution were passed through the membrane. Table I shows the experimental design for the IPN formation.

It was designed a code to identify the modified membranes. This code is made of five characters. The first character is the "M" which stands for membrane, the second one is the monomer concentration (ClVBTA or SSNa), the third one is a number which means the quantity injections of reactive material, the fourth one is the MBA percentage, the fifth one is the "P or 0" which means in presence of functional polymer (P) or in absence of functional polymer (0), and the sixth one is the "Cl^- or Na^+" which means the counterion of the functional group. Both sides of the polypropylene membrane contacted the plasma argon for 1 min using the plasma activation process. Afterward, the active membrane contacted the reactive solution (ClVBTA or SSNa, MBA, and APS). This process was performed

Table I. Experimental Design of the Interpenetrating Polymer Networks (IPN) Synthesis Inside Pores Polypropylene Membranes

Sample code	Monomer (mol L^{-1})	Injections no.	MBA (%)	Plasma activation	Polymer network
M232%0Cl	1.9×10^{-1}	3	2	-	P(ClVBTA)
M432%0Cl	3.8×10^{-1}	3	2	-	
M612%0Cl	5.7×10^{-1}	1	2	-	
M416%0Cl	3.8×10^{-1}	1	6	-	
M418%PCl	3.8×10^{-1}	1	8	-	
M416%PCl	3.8×10^{-1}	1	6	-	
MplasmaCl	3.8×10^{-1}	-	6	1	
M432%0Na	3.8×10^{-1}	3	2	-	P(SSNa)
M416%0Na	3.8×10^{-1}	1	6	-	
M418% PNa	3.8×10^{-1}	1	8	-	
M416% PNa	3.8×10^{-1}	1	6	-	
M414% PNa	3.8×10^{-1}	1	4	-	
MplasmaNa	3.8×10^{-1}	-	6	1	

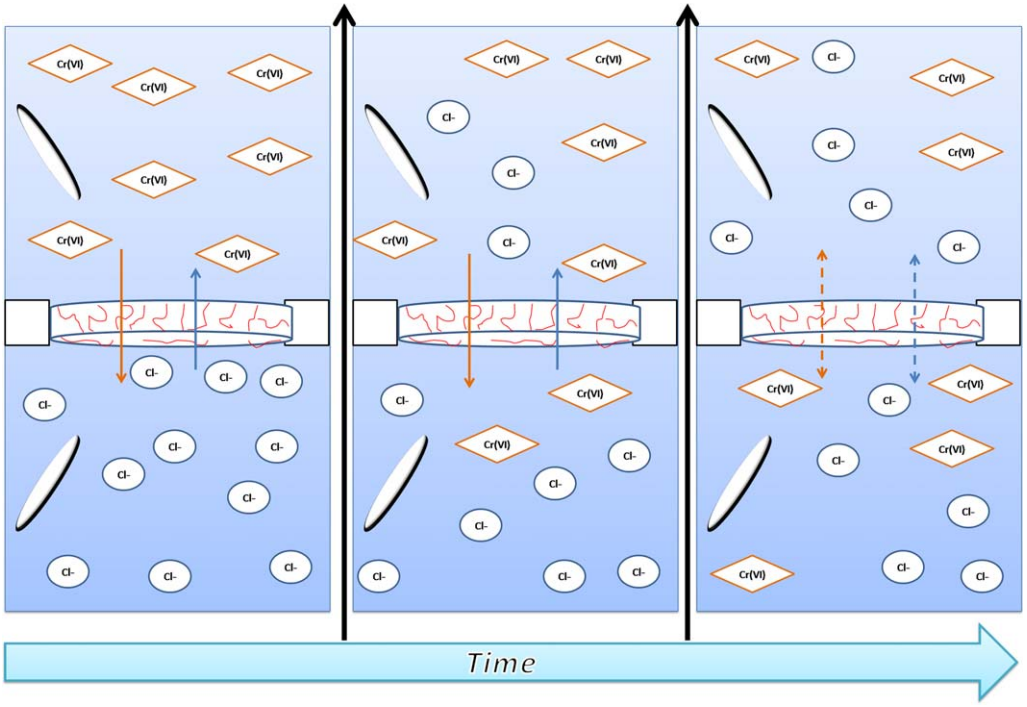

Figure 2. Scheme of a transport cell. [Color figure can be viewed in the online issue, which is available at wileyonlinelibrary.com.]

inside an Erlenmeyer flask under an inert argon atmosphere (see Table I). The samples were identified as MplasmaCl and MplasmaNa. The samples were dried in an oven at 50°C and stored in a silica dryer for 24 h.

Crosslinking the Polyelectrolyte Superficial Layer

M432%0Cl, M612%0Cl, M416%0Cl, M416%PCl, and MplasmaCl, P(ClVBTA) network functionalized membranes were wetted with an aqueous solution of 15 kDa PEI (5% w/w). Similarly, M422%0Na, and M414%PNa, P(SSNa) network membranes were wetted with an aqueous solution of 15 kDa PVA (5% w/w). This wetting process occurred at room temperature for 12 h. The membranes wetted with PEI were submerged in an aqueous Ga (5% w/w) solution. The membranes that were wetted with PVA were contacted with a 1 mol L^{-1} divinylsulfone and sodium carbonate mixture. Both processes were occurred over 12 h to produce the polyelectrolyte crosslinking. Finally, the membranes were washed with water four times. The samples were dried in an oven at 50°C and left in a silica dryer for 24 h. These samples were identified with PEI or PVA added at the end.

CHARACTERIZATION

Modification Percentage

The percent modification was gravimetrically measured. First, the unmodified membranes were weighed. These membrane samples (dry samples) were weighed again after the modification process. The percent modification (% G_M) was determined from the following equation:

$$\%G_M = \frac{(w_f - w_0)}{w_0} \times 100\% \quad (1)$$

where w_f is the dry IPN membrane weight (g), and w_0 is the unmodified membrane weight (g). This method quantitatively calculated the mass percent of the hydrophilic IPN.

Water Uptake Percentage

The weights of the IPN modified membrane dry samples were measured before wetting with distilled deionized water for 24 h. During this period, the samples reached the swelling equilibrium and all tests occurred at room temperature. The excess of water was removed from the modified wet membranes using an absorbent paper in all the tests. The weight of the modified membranes was measured three times due to the membranes are porous. The water uptake percent (%W_w) was calculated from the following equation:

$$\%W_w = \frac{(w_{\text{wet}} - w_{\text{dry}})}{w_{\text{dry}}} \times 100\% \quad (2)$$

where w_{wet} is the wet IPNs membrane weight (g), and w_{dry} is the dry IPN membrane weight (g). This method is gravimetric.

Volumetric Flux

The time required for 50 mL of the distilled deionized water to pass through a modified membrane was measured. A pressure of 1 bar was maintained for all the tests. The equipment used during this step was a stirred-cell filtration unit (Amicon) that works with nitrogen gas. This analysis probes the IPN formation in the pores.

Electrokinetic Properties

Brookhaven ZetaPlus equipment was used. The samples were cut into thin pieces and submerged in 5 × 10^{-2} mol L^{-1} KCl at pH

Table II. Experimental Conditions to Evaluate the Cr(VI) and Cr(III) Ions Transport

Experiment	[Cr(III)] mol L^{-1}	[Cr(VI)] mol L^{-1}	pH-$_{feed\ phase}$	pH-$_{extraction\ phase}$	Extraction agent (mol L^{-1})		Samples
P(ClVBTA)					NaCl		
1	-	5×10^{-4}	3.0	3.0	1		M232%0Cl,
							M432%0Cl,
							M612%0Cl,
							M416%0Cl,
2	-	5×10^{-4}	9.0	9.0	1		M418%PCl,
							M416%.PCl,
							MplasmaCl
P(SSNa)					HNO_3	NaCl	
3	1×10^{-2}	-	2.0	2.0	1×10^{-2}	-	
							M432%0Na,
							MplasmaNa,
4	4×10^{-2}	-	2.0	1.0	1×10^{-1}	-	
							M414% PNa,
							M416% PNa,
5	4×10^{-2}	-	2.0	3.0	1×10^{-3}	-	
							M418% PNa,
							M416%0Na,
6	4×10^{-2}	-	2.0	2.0	1×10^{-2}	1	

3.0, 7.0, and 9.0. The pH was controlled using HCl and NaOH. The electrokinetic potential (ς) was determined from the ionic mobility (μ_e) by using the Smoluchowski Equation [eq. (3)]:

$$\mu_e = \frac{\varepsilon \times \varsigma}{\eta} \tag{3}$$

where μ_e is the ionic electrophoretic mobility ($\mu\ s^{-1}\ V^{-1}$ cm), ε is the liquid permittivity ($J\ V^{-1} \times m^{-1}$), and ς is electrokinetic potential or zeta potential (mV).[45,46] This method determines the electrokinetic potential of the fixed functional groups in the membranes.

Morphological and Microstructural Characterization

Fourier Transform-Infrared Spectroscopy. The Fourier transform-infrared (FT-IR) spectra of the modified membranes were obtained using Nicolet IR-FT equipment with a DTGS-KBr detector (Omnic 5.2 Nicolet instrument Corp.). The measurement occurred between 400 cm^{-1} and 5000 cm^{-1}.

Scanning Electron Microscopy with X-ray Microanalysis. This technique was used to analyze the superficial morphology changes in the modified and unmodified membranes. A 20,000-kV JOEL microscopy (JSH 6380LV model) was used, and an Oxford-instruments INCAx-sight was used for the energy dispersive X-ray spectroscopy (EDS) measurements.

Cr(VI) and Cr(III) Ion Transport Evaluation

A two chamber diffusion cell (feed and extraction phases) was used to evaluate the modified transport membranes. The two chambers were separated by a functional membrane. Figure 2 shows a transport cell working under the Donnan equilibrium principle. Each chamber had a 100-mL capacity and was filled with 50 mL of the work solution for the tests.

Experimental Design. The P(ClVBTA) IPN and P(ClVBTA) modified membranes with a superficial PEI layer were used for Cr(VI) ion transport. Table II shows the experimental conditions for the transport study. The feed chamber was filled with the Cr(VI) solution and the extraction chamber was filled with a 1 mol L^{-1} NaCl solution. Every 60 min for 18–24 h, 3 mL was extracted from the extraction chamber. Direct UV–visible spectrophotometry was used to measure the Cr(VI) ion concentration.[43] The samples were returned to the extraction chamber after reading the Cr(VI) ion concentration.

The P(SSNa) and P(SSNa) IPN membranes with a superficial PVA layer were used to study the Cr(III) ion transport. Table II shows the experimental conditions. The feed chamber was filled with the Cr(III) acid solution, and the extraction chamber was filled with the HNO_3 solution. In other experiments, the extraction chamber was filled with a mixture of 1 mol L^{-1} NaCl and 1×10^{-2} mol L^{-1} HNO_3. Samples were taken from the extraction chamber to measure Cr(III) ion concentration. A 3 mL sample was taken every 60 min for 4 and 6 h. Direct UV–visible spectrophotometry was again used to measure the Cr(III) ion concentrations.[43] The samples were returned to the extraction chamber after reading the Cr(VI) ion concentration.

Binary System. A binary Cr(VI)/NO_3^- solution (1 : 1) was prepared. The Cr(VI) ion source was 5×10^{-4} mol L^{-1} $K_2Cr_2O_7$. The NO_3^- ion source was 1×10^{-1} mol L^{-1} $NaNO_3$, and the solution pH was 9.0. The transport was analyzed using the P(ClVBTA) IPNs membranes. The extraction reagent was 1 ×

Table III. Optimum Values of Modified Degree Percentage, Water Uptake Percentage, Volumetric Flow Change and Extraction Percentage of Cr(VI) and Cr(III) Ions

				%*E* (Cr(VI))		%*E* (Cr(III))	
Sample code	%ΔGM	$\%W_W$	Volumetric flux rate [L×(m^{-2}×h^{-1})]	pH 3.0	pH 9.0	pH 1.0 HNO_3	pH 1.0 HNO_3/NaCl
M232%0Cl	2.6	22.79	62.64	18.3	22.4	-	-
M432%0Cl	3.99	20.3	60.19	32.12	31.51	-	-
M612%0Cl	5.27	15	43.2	35.40	34.95	-	-
M416%0Cl	3.5	15.04	36.86	29.12	38.04	-	-
M418%PCl	3.38	22.54	54.51	15	30	-	-
M416%PCl	4.38	13.20	43.92	30.20	42.01	-	-
MplasmaCl	4.1	12.5	38.50	24.40	59.24	-	-
M432%0Na	3.36	28.4	72.66	-	-	20.59	29.43
M416%0Na	2.74	19.1	35.11	-	-	22.87	32.66
M418%PNa	3.19	18.57	43.57	-	-	15	18
M416%PNa	2.81	16.7	49.14	-	-	20	25
M414%PNa	3.52	19.53	38.74	-	-	28.79	41.14
MplasmaNa	3.53	20.4	40	-	-	34.55	49.36
MPP	-	-	90.30	9.6	21.9	11.22	11.23

10^{-1} mol L^{-1} NaCl at pH 9.0. Every 60 min for 18–24 h, 3 mL of the solution was extracted from the extraction chamber. The Cr(VI) and NO_3^- ion concentrations were determined via UV–visible spectrophotometry. A wavelength of 301 nm was used to determine the NO_3^- ion concentration, and 372 nm was used for Cr(VI).[43]

Transport Evaluation. The transport of Cr(III), Cr(VI), and NO_3^- ions was evaluated based on the extraction percentage (% *E*) calculated using the following equation:

$$\%E = 100 \times \left(\frac{v_e \times c_{i,t}^e}{v_f \times c_{i,0}^f} \right) \quad (4)$$

where V_e and V_f (L) are the extraction chamber and feed chamber volumes, respectively, and $c_{i,t}^e$, is the ion concentration in the extraction chamber, which changes with time. Thus, $c_{i,0}^f$ was the ion concentration in the feed chamber at time of 0, and *E* could be Cr(VI), Cr(III), or NO_3^-.

RESULTS AND DISCUSSION

Synthesis and Characterization of the Functionalized Microporous PP Membranes with Interpenetrated Hydrophilic Polymer Networks

Figure 1 shows the general process for the "*in situ*" synthesis the P(ClVBTA) and P(SSNa) IPNs. The modified evaluation of the modified MPP membranes must consider the changing modification percent and water absorption capacity. These samples were compared to a unmodified microporous polypropylene MPP sample.

The M232%0Cl and M432%0Cl membranes had increasing percent modifications, because it is a function of the injection number and monomer concentration, but if the monomer concentration is 6 mol L^{-1} (M612%0Cl), only is necessary one injection. The percentage of water uptake and change in volumetric flux decreased for these membranes because the P(ClVBTA) IPN grew inside the pore and produced resistance to the water. The percentage of modification for the M432%0Na membrane was similar to the P(ClVBTA) IPN membrane; however, their water uptake percentages and water volumetric fluxes differed. Table III shows these results. It can be attributed to the P(SSNa) IPN morphology in the layer shape, this result will be shown in the SEM analysis. The percentage of modification of the M432%0Cl and M432%0Na membranes were similar, while their water uptake and volumetric fluxes were smaller for higher injection quantities (see Table III). The P(ClVBTA) IPNs formed agglomerated amorphous particles, this will be also shown in the SEM analysis.

The highest percent modification for the IPN membranes with the change in the monomer concentration and the injection number was achieved for the M612%0Cl (5.27%), while that the semi-IPN membranes was achieved high percent modification for the M416%PCl (4.38%), the IPN with the change in the MBA percent was achieved for the M416%0Cl (3.5%), and MplasmaCl (4.1%). Also, the highest percent modification for all of the synthesized P(SSNa) IPN membranes was achieved for MplasmaNa (3.53%), M414%PNa (3.52), and M432%0Na (3.36%). However, the water volumetric flux changes were small relative to the unmodified MPP membrane and close to those of the membranes described in Table III.

The percent uptake and change in the volumetric flux of water by the modified membranes were low relative to the MPP sample. The membranes synthesized via a superficial activation plasma technique (MplasmaCl and MplasmaNa) exhibited percentages of modification, percentage of water uptake, and water volumetric flux changes similar to those for the semi-IPN membranes (M416%PCl and M414%PNa; see Table III).

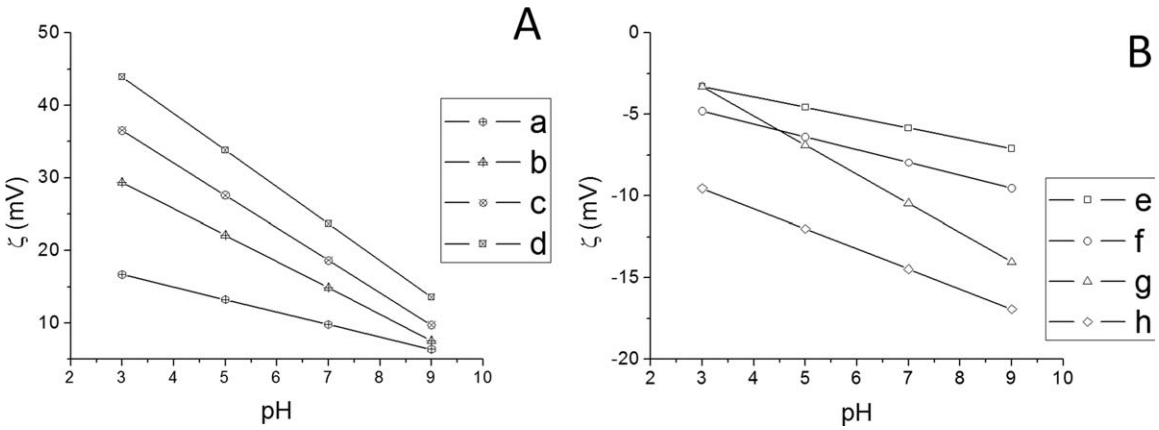

Figure 3. Electrokinetic potential of modified membranes. (A) P(ClVBTA) IPN membranes (a, M416%0Cl; b, M416%PCl; c, MplasmaCl; d, M612%0Cl). (B) P(SSNa) IPN membranes (e, M416%0Na; f, M416%PNa; g, M432%0Na; h, MplasmaNa).

The P(SSNa) was deposited into the PP membrane structure deeper than the P(ClVBTA). The P(ClVBTA) IPNs agglomerated in large quantities on the surface, which makes easier accessing the quaternary ammonium groups.

Electrokinetic Properties

The electrokinetic potential was used to analyze the superficial charge distributions produced by the ionic functional groups. That is to say that electrokinetic potential is the fixed charge potential difference (quaternary ammonium and sulfonate groups) between the mobile ionic charges in the absorption layer.[47] The membrane stability, polyvalent ion absorption capacity, and pore size can be evaluated using the electrokinetic potential.[48,49]

The functional groups in the P(ClVBTA) and P(SSNa) were electrically charged across the entire pH rate.[49,50] The MPP membrane is hydrophobic without any modification and has no ionic functional groups, which renders the membrane inert to electrical fields.

Figure 3 shows the electrokinetic potential behavior. If the functional IPN concentration is high, then the water uptake percent is low because the hydrophobic character increased, and the superficial charges inside the membrane cannot be reaching by the ionic solution. The change in the pH values produced that the IPNs can extend or compacted their segments. The electrokinetic potential values depend of the before behavior described.[51] The P(ClVBTA) IPN membranes exhibited high electrokinetic potentials when the pH was 3.0 [see Figure 3(A)]. These results depend on the excess H^+ repelling the quaternary ammonium groups. The presence and movement of the Cl^- counterion in the diffusion layer becomes favored when the pH is 3.0. At a pH of 9.0, the electrokinetic potential decreases due to OH^- ions. These OH^- ions compete with the Cl^- ions in the diffusion layer. These results depend on the P(ClVBTA) and P(SSNa) IPN concentrations.[52,53] MplasmaCl [see Figure 3(A) c] and M612%0Cl [see Figure 3(A) d] achieved high values of the electrokinetic potential.

The P(SSNa) IPN membranes exhibited the most negative electrokinetic potential value when the pH was 9.0 [see Figure 3(B)]. The excess OH^- ions repelled the sulfonate groups fixed in the network and favored the presence and movement of the Na^+ counterion in the diffusion layer. When the pH was 3.0, the electrokinetic potential becomes less negative because H^+ ions compete with the Na^+ ions in the diffusion layer. These results depend on the P(SSNa) IPN concentrations. M432%0Na

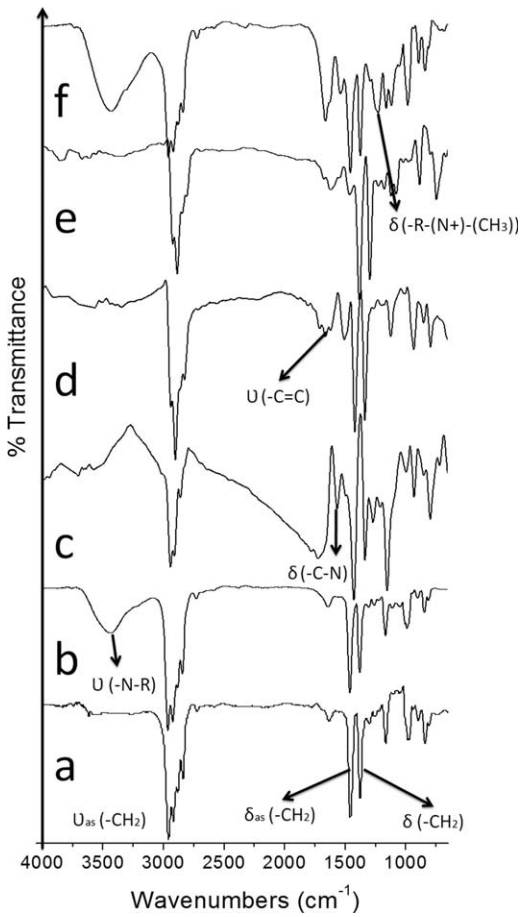

Figure 4. FT-IR spectra of unmodified PP membrane and P(ClVBTA) IPN membranes. (a) MPP. (b) MplasmaCl. (c) M232%0Cl. (d) M432%0Cl. (e) M416%PCl. (f) M418%PCl.

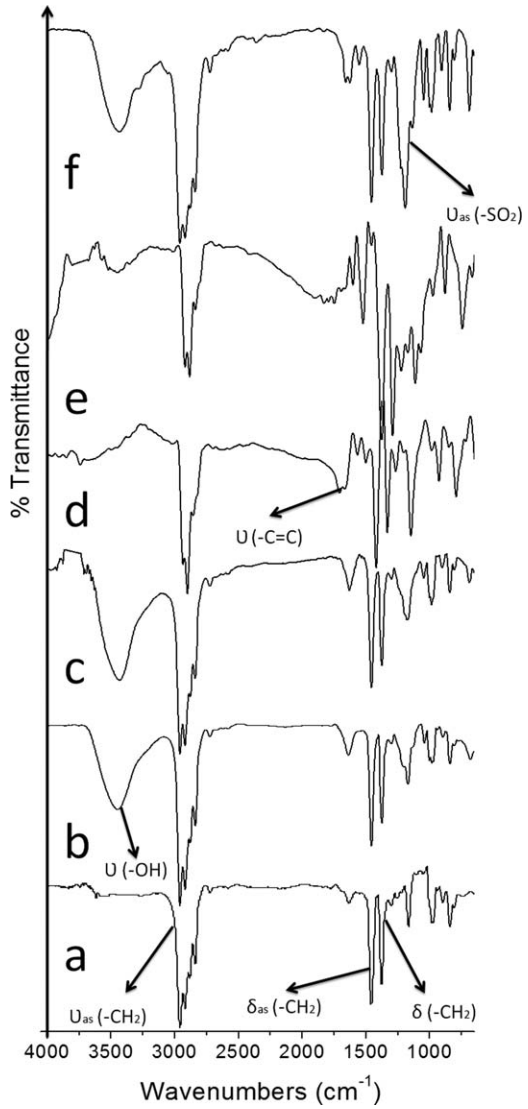

Figure 5. FT-IR spectra of unmodified PP membrane and P(SSNa) IPN membranes. (a) MPP. (b) MplasmaNa. (c) M432%0Na. (d) M416%0Na. (e) M414%PNa. (f) M418%PNa.

[see Figure 3(B) g] and MplasmaNa [see Figure 3(B) h] reach low values of the electrokinetic potential in comparison with the other test samples.

FT-IR Analyses

The microstructural analysis of the modified MPP membranes determined the FT-IR absorption bands corresponding to the functional groups (see Figures 4 and 5).

The FT-IR spectrum for MPP (in cm^{-1}) shows characteristic signals, which were identified, and superficial functional groups belonging to the IPNs. The unmodified PP membrane had characteristic absorption bands at 2970–2800 cm^{-1} corresponding to the stress and asymmetric stretching of C–H (δ_{as}) bonds in the ($-CH_3$) methyl groups. The peak at 1480–1380 cm^{-1} results from the C–H (δ_{as}) of CH_2 bond flexion vibrations because these bonds have asymmetric scissor deformations. The symmetric interaction flexion vibrations for the C–H (δ_s) in the CH_3 bonds were generated across the same range. The signals from 1300 to 700 cm^{-1} represent the changing isotactic polypropylene microstructural characteristics. The signals at 1200, 1116, 998, 841, and 800 cm^{-1} are the isotactic configuration crystallinity sequences.[54] The signal at 970 cm^{-1} corresponds to the monomeric head-to-tail isotactic polypropylene configuration.[55] Figures 4(a) and 5(a) show the MPP FT-IR spectra.

The signals representing the P(ClVBTA) IPN membranes are the aromatic C═C absorption signals occur in the range from 1400 cm^{-1} to 1600 cm^{-1}; the quaternary ammonium group has the absorption signals at 1581 cm^{-1} for the N–H bond and C–N vibration and 1483 cm^{-1} for the [$-N^+-(CH_3)$] group bond flexion. Figure 4(b) shows the signals of the MplasmaCl, Figure 4(c) to M232%0Cl. Figure 4(d) to M432%0Cl, Figure 4(e) to M416%PCl. Figure 4(f) to M418%PCl. However, the M232%0Cl, M416%PCl, and M418%PCl show very well the signals of the quaternary ammonium, while that the M232%0Cl, M432%0Cl, M416%PCl, and M418%PCl produce pronounced signals of the aromatic group. These results are possible due to the functional networks onto the surface polypropylene fibers.

Also, it was analyzed the characteristic absorption signals for the P(SSNa) IPN membranes. For example, the SO_3^- from the sulfonate group was observed at 1042 cm^{-1} (S═O) and 1175 cm^{-1}, while the peaks at 1400–1600 cm^{-1} corresponded to the aromatic (C═C)carbons. Figure 5(b) shows the signals of the MplasmaNa, Figure 4(c) to M432%0Na, Figure 4(d) to M416%0Na, Figure 4(e) to M414%PNa, and Figure 4(f) to M418%PNa. All samples with P(SSNa) IPNs show the signals of the sulfonate groups and –OH, but only M416%0Na, M414%PNa and M418%PNa have very well the signals of the aromatic group.

The C–H and C–C bonds were observed in the spectra for the modified and unmodified MPP membranes. These signals are stronger in the modified membrane than the unmodified MPP membrane. The absorption signals [ϑ_{as} ($-CH_2$), δ_{as} ($-CH_2$), and δ_s ($-CH_2$)] were stronger in the modified membrane samples than the unmodified PP membrane signs (see Figures 4 and 5).

SEM Analyses of the Morphologic Changes

Figure 6 shows the morphology of unmodified microporous MPP, and IPN membranes. Figure 6(a,b), of the membrane face had an intertwined fiber structure, low porosity, and smooth superficial aspect. Figure 6(c) shows high density based on the thick, compacted polypropylene fiber group. These results represent an anisotropic membrane.[56,57] The membrane morphology changes for the P(ClVBTA) and P(SSNa) IPN membranes were compared to the unmodified MPP membrane.

M416%0Cl membrane SEM images are show in Figure 6(d–f). Two different phases were observed, the first is the polypropylene fibers and the seconds is the P(ClVBTA) networks. The polypropylene fibers provide support and mechanical resistance to the amorphous IPN materials [see Figure 6(d)], while the IPN materials produced the ion exchange. These results indicate a change in the microstructural homogeneity [see Figure 6(e)] compared to the unmodified MPP membrane [see Figure

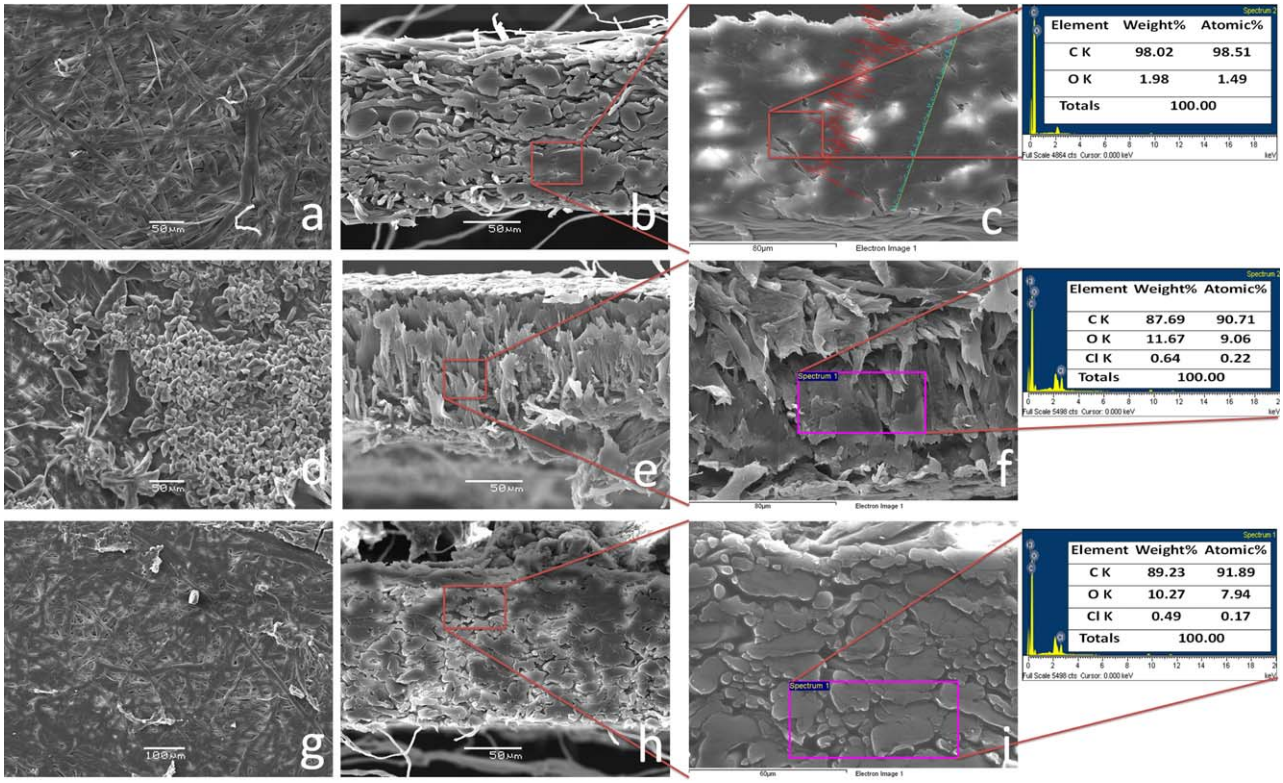

Figure 6. SEM/EDS images of the P(ClVBTA) IPN microporous membranes to 50 μm, and ×300. Unmodified MPP membrane (a, upper face; b, down face; c, cross-section area). M416%0Cl membrane (d, upper face; e, cross-section area; f, EDS image with 80 μm, and ×180). M418%PCl membrane (g, upper face with 100 μm, and ×100; h, cross-section area; i, EDS image with 60 μm, and ×260). [Color figure can be viewed in the online issue, which is available at wileyonlinelibrary.com.]

6(a,c)]. The EDS elemental analysis was obtained from the cross-sectional area [see Figure 6(f)] and measured the elemental concentration for the Cl^- counterion. Also, it was analyzed the M418%PCl membrane [see Figure 6(g–i)]. It is possible to observe two different phases lesser amount than the M416%0Cl in the Figure 6(g). The morphology of M416%0Cl and M418%PCl membranes was compared because the P(ClVBTA) lineal polymer could produce one effect onto the interpenetrating polymer networks forming. The cross-section area [see Figure 6(h)] of the M418%PCl is more similar to the MPP [see Figure 6(c)]. It is probable that, the high hydrophobic character produce a separation of the phases between the P(ClVBTA) and the polypropylene, due to the 8% of the MBA and the presence of the P(ClVBTA) lineal. Figure 6(i) shows the EDS of the cross-sectional area part, and indicates the Cl^- counterion presence.

This indirect method probed the quaternary ammonium group in the P(ClVBTA) IPN. The highest P(ClVBTA) IPN concentration was found on the superficial face relative to the observed membrane cross-section.

Previous research has similar results to this investigation according to the morphology of the functional polymers inside the porous membranes using SEM. For example, the grafted and copolymerized 4-vinylpiridinium monomer within MPP membranes, and, they reach a pore-narrowing and pore-blocking; the smoother surface cover by a thin polymer layer; and surface membranes evenly modified.[58] The morphology of these membranes are very similar to the morphology achieved in this investigation (P(ClVBTA) IPNs). Due to that it is possible to observe some places with the amorphous materials of the functional polymer. Another study shows that the poly(*N*,*N*-dimethylaminoethyl methacrylate) (PDMAEMA) was grafted and crosslinked onto the MPP membrane surface. The results show that the membrane surfaces were covered by the functional polymer layer. However, at low concentration of the polymer network, the layer almost homogeneously and does not change the porosity of the polypropylene supports.[59]

M416%0Na membrane morphology is showing in the Figure 7(a–c). Also, this membrane exhibited 2 phases relative to the unmodified MPP membrane [see Figure 7(a)]. These phases are the polypropylene support that is the initial material, and the other is the functional polymer network enclosed in the structure of MPP, in this case it is P(SSNa). The P(SSNa) IPN particle sizes were smaller and less agglomerated than the P(ClVBTA) IPNs [see Figure 7(b)]. The P(SSNa) IPNs covered the entire MPP fiber surface like a paint. An EDS elemental analysis on the cross-sectional area of the M416%0Na membrane detected sodium and sulfur belonging to the sulfonate group [see Figure 7(c)]. Furthermore, M416%PNa was tested with the SEM [see Figure 7(d–f)]. This membrane shows 2 phases (P(SSNa) covering the polypropylene fibers) in its structure principally onto the surface [see Figure 7(d)]. In the cross-

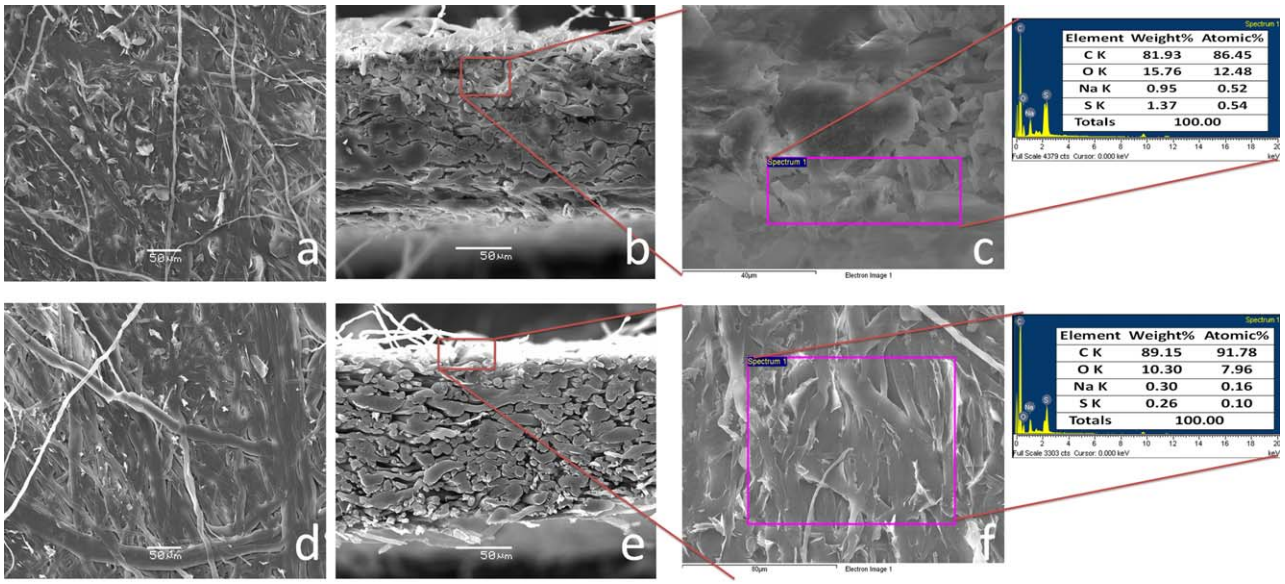

Figure 7. SEM/EDS images of the P(SSNa) IPN microporous membranes to 50 μm, and ×300. M416%0Na membrane (a, upper face; b, cross-section area; c, EDS image with 40 μm, and ×517). M416%PNa membrane (d, upper face; e, cross-section area; f, EDS image with 80 μm, and ×180). [Color figure can be viewed in the online issue, which is available at wileyonlinelibrary.com.]

section area this membrane keeps the same morphology than the MPP sample [see Figures 6(c) and 7(e)]. The P(SSNa) IPNs is not easy identify in this part, possibly these materials are mixed with the polypropylene fibers. It is more easy observed the P(SSNa) on the surface of the membranes, it is the same case by the P(ClVBTA) IPNs. Hence, the EDS was made on the surface membrane [see Figure 7(f)], and it was detected sulfur and sodium elemental, together with the some IPN materials.

The P(SSNa) IPNs were better distributed relative to the P(ClVBTA) IPN, and the P(SSNa) IPNs were smaller relative to the P(CLVBTA) IPNs. The P(SSNa) IPNs tended to be more homogeneous and cover more PP fibers than the P(ClVBTA) IPNs.

The literature shows similar SEM results for the surface and cross-sectional area of modified PVDF membranes with P(SSNa) grafted into their superficial fibers and pore walls.[60] Similar results were obtained when a polypropylene film was superficially modified with P(SSNa) and a polyethylene film was modified with P(SSNa). The main results found a structural surface change where small particles with small pores appeared.[61]

In general, the membranes exhibited low IPN concentrations in their cross-sections due to the hydrophobic nature of the isotactic MPP and low pore uniformity due to their high asymmetric character.[62,63] These results are indicating that the membrane surface has been unevenly modified.

Cr(VI) and Cr(III) Ions Transport Evaluation

Analysis of the P(ClVBTA) Networks Response. The transport capacity for Cr(VI) ions through PP membranes modified with IPNs and semi-IPNs P(ClVBTA) was evaluated. Membranes modified with the IPNs and semi-IPNs P(SSNa) were used for Cr(III). The Cr(VI) and Cr(III) concentrations are suitable for the interaction with the fixed charges in the membrane.[64] The Cr(VI) ion species in an acid environment (pH 3.0) primarily form $Cr_2O_7^{2-}$ and $HCrO_4^-$ depending on the concentration.[2,65] At pH 9.0 most of the Cr(VI) ions are CrO_4^{2-}.

The percent extractions decreased from M612%0Cl (35.40%)>M416%PCl (30.20%)> M416%0Cl (29.12%) >MplasmaCl (24.40%) > MPP (9.6%) at pH 3.0, and the values are shown in Table III with the membranes containing the semi-(INP)s M416%PCl, and M612%0Cl. The MplasmaCl membrane exhibited a lower percent extraction than the membranes containing P(ClVBTA) (IPN)s.

Figure 8(A) shows the percent Cr(VI) ion extraction for membranes modified with P(ClVBTA) at pH 3.0 compared to the unmodified MPP membrane wetted with ethanol.

The membranes synthesized via the plasma method represent a superficial modification and cannot change the membrane thickness. The extraction values for the membranes with a 15 kDa PEI superficial are from the highest to the lowest, M416%0Cl.PEI [35.8%; see Figure 8(A) a] > M416%PCl.PEI (32.9%) > M612%0Cl.PEI (32.2%) > MplasmaCl.PEI [30.7%; see Figure 8(A) b]> MPP.PEI (13.0%) > MPP (9.6%). These values are higher than those for the P(ClVBTA) IPN membranes without a PEI superficial layer. The PEI was absorbed on the membrane surface to form a monolayer.[66]

At a pH of 3.0, the PEI monolayer becomes charged with a hydrogen ion that reinforces the Cr(VI) ion interactions with the cationic groups. The PEI monolayer obstructs the smallest pores and partially obstructs bigger pores due to the electrostatic repulsion between the protonated amines and quaternary ammonium groups.[66]

Usually, the Cr(VI) ion transport under such conditions depends on the P(ClVBTA) network concentration. In addition,

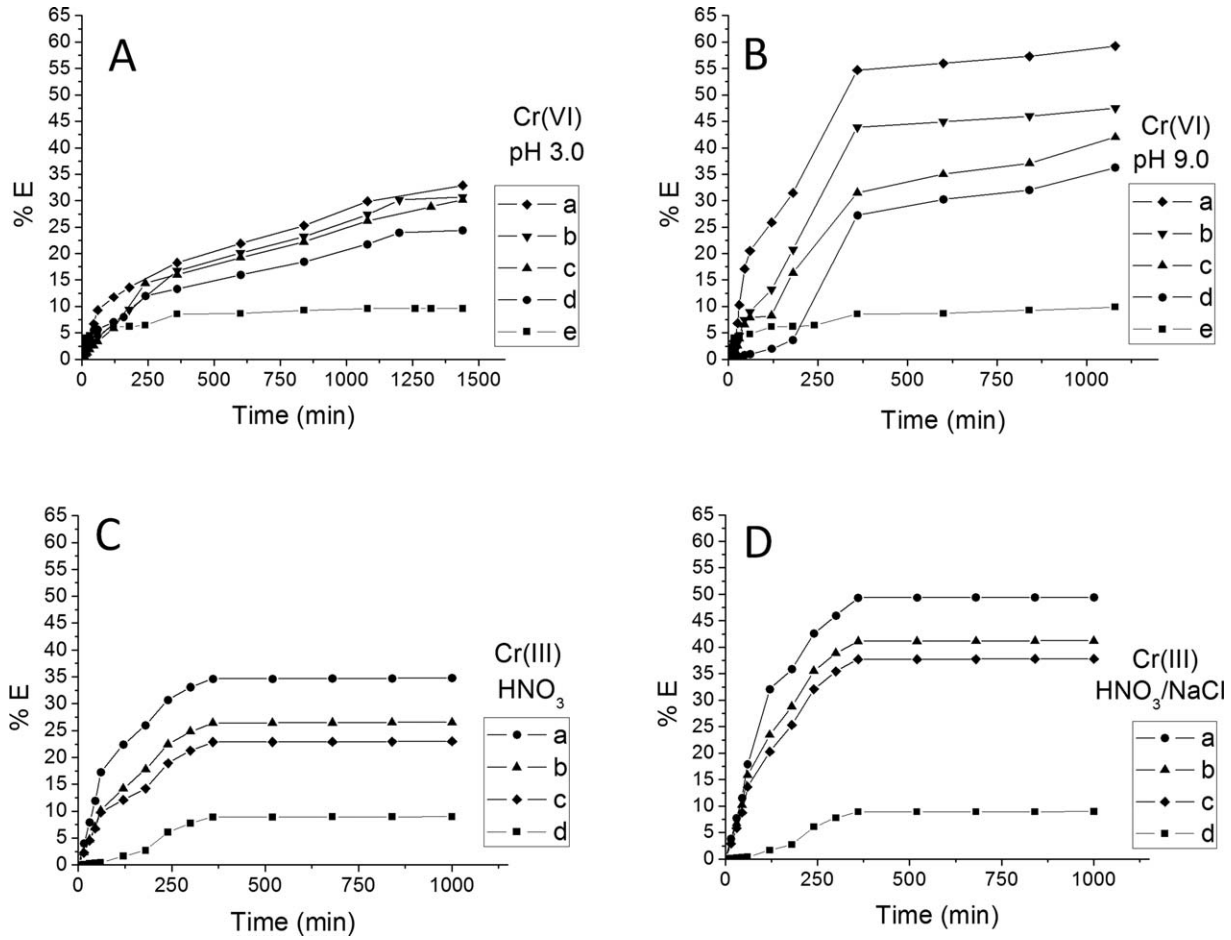

Figure 8. Extraction profile. (A) Membranes (a, M416%PCl.PEI; b, MplasmaCl.PEI; c, M416%PCl; d, MplasmaCl; e, MPP) for Cr(VI) ions. (B) Membranes (a, MplasmaCl; b, MplasmaCl.PEI; c, M416%PCl; d, M416%PCl.PEI; e, MPP) for Cr(VI) ions. (C) Membranes (a, MplasmaNa; b, M414%PNa.PVA; c, M414%PNa; d, MPP) for Cr(III) ions. (D) Membranes (a, MplasmaNa; b, M414%PNa; c, M414%PNa.PVA; d, MPP) for Cr(III) ions.

this concentration influences the membrane synthesis method, which is the pressure injection method. In the same way, a strong quaternary ammonium group interacts with the dichromate ions, which decreases the ion exchange velocity and increases the ion exchange relationship.[66]

The Donnan equilibrium was achieved after 1000 min. Figure 8(B) shows the Cr(VI) ion extraction profile (at pH 9.0) for membranes modified with the P(ClVBTA) networks. The obtained percent extractions for the Cr(VI) ion were, in order, MplasmaCl [59.24%; see Figure 8(B) a] > M416%PCl (42.01%) > M416%0Cl (38.04%) > MPP (11.57%). The membranes containing a 15 kDa PEI superficial layer exhibited the following orderingMplasmaCl.PEI [47.54%; see Figure 8(B) b] > M416%PCl.PEI (36.28%) > MPP (21.9%) > MPP.PEI (16.4%). These results are shown in Table III. The Cr(VI) ion at a pH of 9.0 yielded higher percent extraction than at a pH of 3.0.

These Cr(VI) ions compete against hydroxyl ions during ion exchanges within the membrane. The reason this competition occurs is because the membrane has quaternary ammonium groups with positive charges. The transfer of Cr(VI) is higher at pH 9.0 than at pH 3.0 because the$Cr_2O_7^{2-}$ Stokes radii is higher than the CrO_4^{2-} Stokes radii. This size difference causes friction during the movement and a strong electrostatic force during the ion exchange. The Stokes radii and Gibbs free energies are shown in Table IV.

Because the $Cr_2O_7^{2-}$ ions are more hydrated, they have a larger volume and interact with the quaternary ammonium groups and protonated amines. All of these traits produce a retention

Table IV. Stokes Radii (nm) and Gibbs Hydration Energies of Various Ions[51,53]

Ion	$-\Delta G_f^0$ (kJ mol^{-1})	Radium of stokes (nm)
$Cr_2O_7^{2-}$	1301.1	0.297
Cl^-	317	0.168
NO_3^-	270	0.2
H^+	1050	0.030
CrO_4^{2-}	950	0.240
Cr^{3+}	4010	0.062
Na^+	365	0.102
OH^-	465	0.133

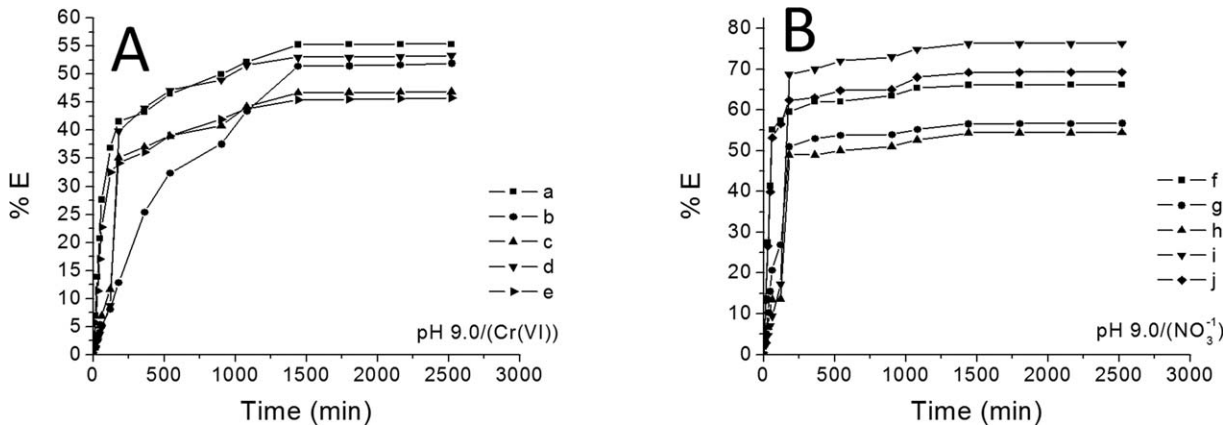

Figure 9. Extraction profile for binary system at pH 9.0. (A) Membranes (a, M612%0Cl.PEI; b, M416%0Cl.PEI; c, M416%PCl; d, M416%PCl.PEI; e, M612%0Cl) for Cr(VI) ions. (B) Membranes (f, M612%0Cl.PEI; g, M416%0Cl; h, M416%PCl; I, M416%.PCl.PEI; j, M612%0Cl) for NO_3^- ions.

effect. At pH 9.0, the PEI monolayer is not charged and produces a chelating effect due to the concentration gradient when the Cr(VI) ions and quaternary ammonium groups or Cr(VI) ions and amine groups interact during the diffusion.

Analysis of the P(SSNa) Networks Response. Figure 8(C) shows the results from the Cr(III) ion extraction for the P(SSNa) IPN and superficial 15 kDa PVA layer over the membranes. The extractor agent was 1×10^{-1} mol L^{-1} HNO_3. The experiments were conducted in an acidic solution. The acidity guarantees the total dissolution and Cr(III) ionization, which avoids forming metallic hydroxyls.[67]

The Donnan equilibrium was obtained after 350 min; however, this value may depend on the strong ionic interactions between the Cr(III) ions and membrane sulfonate groups. The P(SSNa) network membranes yielded percent Cr(III) extractions decreasing from MplasmaNa (34.55%) [see Figure 8(C) a] > M414%PNa (28.79%) > M416%0Na (22.87%) > M432%0(20.59%) > MPP (11.22%). All of these results are shown in Table III. The superficial 15 kDa PVA layer membranes were obtained in the following order: M432%0.PVA (34.65%) > M414%PNa.PVA [26.39%; see Figure 8(C) b] > MPP (11.22) > MPP.PVA (6.43%). The PVA may not chelate, and the pores sizes did not decrease. The PVA improved the hydrophilicity of the P(SSNa) network membranes.

Figure 8(D) shows the percent Cr(III) ion extraction profiles using a mixture of 1×10^{-1} mol L^{-1} HNO_3 and 1 mol L^{-1} NaCl as the extractor reagent. This mixture improved the Cr(III) transport relative to using HNO_3 alone. The high sodium ion concentration in the extractor mixture may exchange with the Cr(III) ions and stimulates both ion diffusion due to the concentration gradient.[68,69] The percent extraction membrane were ordered as MplasmaNa [49.36%; see Figure 8(D) a] > M414%PNa [41.14%; see Figure 8(D) b] > M416%0Na(32.66%) > M432%0Na (29.43%) > MPP (11.23%). The superficial PVA layer P(SSNa) membranes were M432%0Na.PVA (49.51%) > M414%PNa.PVA (37.71%) > MPP (11.23%) > MPP.PVA (7.77%). The H^+ ion has a higher movement capacity during the membrane phase because of its small size (see Table IV) relative to the Cr(III) size.

Breaking the ion exchange equilibrium and separating the Cr(III) ions from the sulfonate groups requires a strong ionic or acidic force. Therefore, the NaCl improved the Cr(III) movement and transport into the extraction phase.

Analysis of the P(ClVBTA) Networks Response in a Binary System. Figure 9 shows the percent extraction for a binary compound system containing Cr(VI) and NO_3^- ions. The P(ClVBTA) network and superficial PEI layer membranes were used in this system for a solution at pH 9.0. The extraction reagent was 1 mol L^{-1} NaCl.

The Donnan equilibrium for the Cr(VI) ions was achieved between 250 min and 500 min [see Figure 9(A)]. However, the Donnan equilibrium for the NO_3^- ions was reached between 250 min and 340 min [see Figure 9(B)].

The Cr(VI) ions extraction behavior after using the P(ClVBTA) networks were M612%0Cl.PEI [see Figure 9(A) a] > M416%PCl.PEI [see Figure 9(A) b] > M416%0Cl.PEI > M416%PCl > M612%0Cl > M416%0Cl, while those for the NO_3^- ions %PCl.PEI [see Figure 9(B) f] > M612%0Cl [see Figure 9(B) g] > M612%0Cl.PEI > M416%0Cl > M416%PCl. The percent extraction was between 50% and 60% for Cr(VI) and between 50% and 70% for NO_3^-.

These results may be due to the differences between the Stokes radii and Gibbs free-energy for hydration as shown in Table IV. The NO_3^- ions were smaller and less hydrated than the Cr(VI) ions, which provides more movement through the membranes. The quaternary ammonium groups preferred the Cr(VI) ions because they are divalent.

CONCLUSIONS

Microporous polypropylene membranes with ion exchange capacities can be obtained by synthesizing interpenetrating polymer networks (IPNs) using radical polymerization. The reactive mixture was injected by pressure, or the membrane surfaces were activated via an argon gas plasma activation. The functional monomer and crosslinked MBA concentrations play important roles in (IPN) membranes synthesized "*in situ*" because they can control the network density.

The properties of the polypropylene membranes with P(ClVBTA) and P(SSNa) IPNs were evaluated via hydrophilicity capacity, SEM/EDS, FT-IR, and electrokinetic studies. These

results demonstrated the IPNs form within the pores. The modified membranes were compared to the unmodified PP membranes.

The transport properties for the Cr(VI) and Cr(III) ions were evaluated using the Donnan dialysis principle. The Cr(VI) extraction results using the M416%0.PEI and MplasmaCl tested at acidic pH and basic pH. The M416%0.PEI membrane was selected because the obtention of Cr(VI) ions transport results (35.80%) at pH 3.0. The MplasmaCl membrane was selected due to its transport capacity (52.24%) for Cr(VI) ions at pH9.0.

The P(SSNa) (IPN) membranes were used as Cr(III) ion transports when the MplasmaNa (34.35%)was selected for the 1×10^{-1} mol L^{-1} HNO_3 extraction reagent, and the M432%0Na.PVA (49.51%) membrane was selected when the extraction agent was a 1×10^{-2} mol L^{-1} HNO_3 and 1 mol L^{-1} NaCl mixture.

The polypropylene membranes modified with P(ClVBTA) or P(SSNa) IPNs were valued in terms of their economy, simplicity, and synthesis time. The Cr(VI) and Cr(III) extraction results were also important because the starting material was initially hydrophobic, and the wetting properties improved upon modification.

ACKNOWLEDGMENTS

The authors thank the FONDECYT (Project No 1110079), PIA (Anillo ACT-130), 7FP-MC Actions Grant, CHILTURPOL2 (PIRSES-GA-2009 Project, Grant No: 269153), REDOC (MINEDUC Project UCO1202 at U. de Concepción), and Marie Curie Program. Julio Sánchez thanks FONDECYT (Project No 11140324) and CIPA, Chile.

REFERENCES

1. Ahmed, M. E. I. *Eleventh International Water Technology Conference*, **2007**, 233.
2. Owlad, M.; Aroua, M. K.; Daud, W. A. W.; Baroutian, S. *Water Air Soil Poll.* **2009**, *200*, 59.
3. WHO, Guidelines for Drinking-Water Quality, World Health Organization, Geneva, **1993**.
4. Mielenz, K. D.; Velapoldiand, R.; Mavrodineanu, R. *Standardization in Spectrophotometry and Luminescence Measurements: Proceedings of a Workshop Seminar Held at the National Bureau of Standards, Gaithersburg, Maryland, November, November 19–20, 1975*, US Department of Commerce, National Bureau of Standards, **1976**.
5. Sardohan, T.; Kir, E.; Gulec, A.; Cengeloglu, Y. *Sep. Purif. Technol.* **2010**, *74*, 14.
6. Refugio Bernardo, G.-R.; Jose Rene, R.-M.; Ma Catalina, A.-D. l. T. *J. Hazard Mater.* **2009**, *170*, 845.
7. Richardand, F. C.; Bourg, A. *Water Res.* **1991**, *25*, 807.
8. Golder, A.; Samanta, A.; Ray, S. *Sep. Purif. Technol.* **2007**, *53*, 33.
9. Sánchez, J.; Rivas, B. L. *Desalination* **2011**, *279*, 338.
10. Patterson, R. R.; Fendorf, S.; Fendorf, M. *Environ. Sci. Technol.* **1997**, *31*, 2039.
11. Park, D.; Lim, S.-R.; Yun, Y.-S.; Park, J. M. *Chemosphere* **2007**, *70*, 298.
12. Arslan, G.; Pehlivan, E. *Bioresour. Technol.* **2007**, *98*, 2836.
13. Cavaco, S. A.; Fernandes, S.; Quina, M. M.; Ferreira, L. M. *J. Hazard Mater.* **2007**, *144*, 634.
14. Saravanan, S.; Begum, K. M. S.; Anantharaman, N. *J. UChem. Technol. Metal* **2006**, *41*, 333.
15. Nataraj, S.; Hosamani, K.; Aminabhavi, T. *Desalination* **2007**, *217*, 181.
16. Venkateswaranand, P.; Palanivelu, K. *Hydrometallurgy* **2005**, *78*, 107.
17. Bhowal, A.; Datta, S. *J. Membr. Sci.* **2001**, *188*, 1.
18. Cwirko, E. H.; Carbonell, R. G. *J. Membr. Sci.* **1990**, *48*, 155.
19. Tor, A.; Çengeloğlu, Y.; Ersöv, M.; Arslan, G. *Desalination* **2004**, *170*, 151.
20. Narębska, A.; Staniszewski, M. *Separ. Sci. Technol.* **2008**, *43*, 490.
21. Zheleznov, A.; Windmöller, D.; Körner, S.; Böddeker, K. *J. Membr. Sci.* **1998**, *139*, 137.
22. Mathur, J.; Murali, M.; Krishna, M. B.; Ramachandhran, V.; Hanra, M.; Misra, B. *J. Radioanal. Nucl. Chem.* **1998**, *232*, 237.
23. Said, A. A.; Amara, M.; Kerdjoudj, H. *Ionics* **2013**, *19*, 177.
24. Dzyazko, Y. S.; Vasilyuk, S. L.; Rozhdestvenskaya, L. M.; Belyakov, V. N.; Stefanyak, N. V.; Kabay, N.; Yüksel, M.; Arar, Ö.; Yüksel, Ü. *Chem. Eng. Commun.* **2008**, *196*, 22.
25. Castillo, E.; Granados, M.; Cortina, J. L. *J. Chromatogr. A* **2002**, *963*, 205.
26. Castillo, E.; Granados, M.; Cortina, J. L. *Anal. Chim. Acta* **2002**, *464*, 15.
27. Thapliyal, P. *Compos. Interfaces* **2010**, *17*, 85.
28. Chikh, L.; Delhorbe, V.; Fichet, O. *J. Membr. Sci.* **2011**, *368*, 1.
29. Merle, G.; Wessling, M.; Nijmeijer, K. *J. Membr. Sci.* **2011**, *377*, 1.
30. Abbasi, F.; Mirzadeh, H.; Katbab, A. A. *Polym. Int.* **2001**, *50*, 1279.
31. Sahiner, N.; Godbey, W.; McPherson, G. L.; John, V. T. *Colloid Polym. Sci.* **2006**, *284*, 1121.
32. Bajpai, A.; Bajpai, J.; Shukla, S. *React. Funct. Polym.* **2002**, *50*, 9.
33. Krajewska, B. *Enzyme Microb. Tech.* **2004**, *35*, 126.
34. M'Bareck, C. O.; Nguyen, Q. T.; Alexandre, S.; Zimmerlin, I. *J. Membr. Sci.* **2006**, *278*, 10.
35. Nagarale, R.; Gohil, G.; Shahi, V. K. *Adv. Colloid Interface* **2006**, *119*, 97.
36. Couture, G.; Alaaeddine, A.; Boschet, F.; Ameduri, B. *Prog. Polym. Sci.* **2011**, *36*, 1521.
37. Rivas, B. L.; Pereira, E. D.; Moreno-Villoslada, I. *Prog. Polym. Sci.* **2003**, *28*, 173.
38. Rivas, B. L.; Aguirre, M. d. C.; Pereira, E. *J. Appl. Polym. Sci.* **2006**, *102*, 2677.

39. Palencia, M.; Rivas, B. L.; Pereira, E.; Hernández, A.; Prádanos, P. *J. Membr. Sci.* **2009**, *336*, 128.
40. Rivas, B. L.; del Carmen Aguirre, M.; Pereira, E. *J. Appl. Polym. Sci.* **2007**, *106*, 89.
41. Rivas, B. L.; Pereira, E. D.; Palencia, M.; Sánchez, J. *Prog. Polym. Sci.* **2011**, *36*, 294.
42. Rivas, B. L.; Pooley, S. A.; Pereira, E. D.; Maureira, A. *Macromol. Symp.* **2006**, 116.
43. Thomasand, O.; Burgess, C. UV-Visible Spectrophotometry of Water and Wastewater; Elsevier: Amsterdam, **2007**.
44. Bryjak, M.; Duraj, I. *Desalination* **2013**, *310*, 39.
45. Szymczyk, A.; Fievet, P.; Reggiani, J.; Pagetti, J. *Desalination* **1998**, *115*, 129.
46. Zhou, J.; Zhang, X.; Wang, Y.; Hu, X.; Larbot, A.; Persin, M. *Desalination* **2009**, *235*, 102.
47. Keand, Y.; Stroeve, P. Polymer-Layered Silicate and Silica Nanocomposites; Elsevier: Amsterdam, **2005**.
48. Szymczyk, A.; Fievet, P.; Reggiani, J.; Pagetti, J. *J. Membr. Sci.* **1998**, *146*, 277.
49. Li, Y.-H.; Wang, S.; Luan, Z.; Ding, J.; Xu, C.; Wu, D. *Carbon* **2003**, *41*, 1057.
50. Kim, D. H.; Moon, S.-H.; Cho, J. *Desalination* **2003**, *151*, 11.
51. Hu, K.; Dickson, J. M. *J. Membr. Sci.* **2008**, *321*, 162.
52. Yu, H.-Y.; Xu, Z.-K.; Yang, Q.; Hu, M.-X.; Wang, S.-Y. *J. Membr. Sci.* **2006**, *281*, 658.
53. Szymczyk, A.; Fievet, P.; Aoubiza, B.; Simon, C.; Pagetti, J. *J. Membr. Sci.* **1999**, *161*, 275.
54. Xinyuan Zhu, D. Y.; Yao, H.; Zhu, P. *Macromol. Rapid Commun.* **2000**, *21*, 354.
55. Pretsch, E.; Bühlmann, P.; Affolter, C.; Pretsch, E.; Bhuhlmann, P.; Affolter, C. Structure Determination of Organic Compounds; Springer: Berlin, **2000**.
56. Ulbricht, M. *Polymer* **2006**, *47*, 2217.
57. Matsuyama, H.; Yuasa, M.; Kitamura, Y.; Teramoto, M.; Lloyd, D. R. *J. Membr. Sci.* **2000**, *179*, 91.
58. Wang, C.-c.; Yang, F.-l.; Liu, L.-F.; Fu, Z.-M.; Xue, Y. *J. Membr. Sci.* **2009**, *345*, 223.
59. Yang, Y.-F.; Wan, L.-S.; Xu, Z.-K. *J. Membr. Sci.* **2009**, *326*, 372.
60. Nasef, M.; Zubir, N.; Ismail, A.; Khayet, M.; Dahlan, K.; Saidi, H.; Rohani, R.; Ngah, T.; Sulaiman, N. *J. Membr. Sci.* **2006**, *268*, 96.
61. Maddanimath, I. S. M. T.; Sainkar, S. R.; Vijayamohanan, K.; Shaikh Patil, K. I.; Vernekar, S. P. *Sensor Actuat. B: Chem.* **2002**, *81*, 141.
62. Yang, Q.; Xu, Z.-K.; Dai, Z.-W.; Wang, J.-L.; Ulbricht, M. *Chem. Mater.* **2005**, *17*, 3050.
63. Schauer, J.; Hnát, J.; Brožová, L.; Žitka, J.; Bouzek, K. *J. Membr. Sci.* **2012**, *401*, 83.
64. Tor, A. *J. Hazard Mater.* **2007**, *141*, 814.
65. Kotaś, J.; Stasicka, Z. *Environ. Pollut.* **2000**, *107*, 263.
66. Sata, T. Ion Exchange Membranes: Preparation, Characterization, Modification and Application; Royal Society of Chemistry: London, UK, **2004**.
67. Wu, D.; Sui, Y.; He, S.; Wang, X.; Li, C.; Kong, H. *J. Hazard Mater.* **2008**, *155*, 415.
68. Marzouk, I.; Dammak, L.; Chaabane, L.; Hamrouni, B. *AM J. Anal. Chem.* **2013**, 4.
69. Cengeloglu, Y.; Kir, E.; Ersoz, M.; Buyukerkek, T.; Gezgin, S. *Colloid Surf. A* **2003**, *223*, 95.